Arabian Journal of Chemistry (2016) 9, 518–525

King Saud University

Arabian Journal of Chemistry

www.ksu.edu.sa
www.sciencedirect.com

ORIGINAL ARTICLE

Optimization of Reactive Blue 21 removal by Nanoscale Zero-Valent Iron using response surface methodology

Mahmood Reza Sohrabi [a], Mina Moghri [a,b,*], Hamid Reza Fard Masoumi [c], Sama Amiri [a], Nasim Moosavi [a]

[a] *Department of Chemistry, Islamic Azad University, North Tehran Branch, P.O. Box 1913674711, Tehran, Iran*
[b] *Young Researchers and Elites Club, North Tehran Branch, Islamic Azad University, Tehran, Iran*
[c] *Department of Chemistry, Faculty of Science, University Putra Malaysia, 43400 Serdang, Selangor, Malaysia*

Received 8 August 2014; accepted 18 November 2014
Available online 18 December 2014

KEYWORDS

Zero-Valent Iron nanoparticles;
Response surface methodology (RSM);
Central composite design;
Reactive Blue 21;
Wastewater

Abstract Since Reactive Blue 21 (RB21) is one of the dye compounds which is harmful to human life, a simple and sensitive method to remove this pollutant from wastewater is using Nano Zero-Valent Iron (NZVI) catalyst. In this paper, a Central Composite Rotatable Design (CCRD) was employed for response surface modeling to optimize experimental conditions of the RB21 removal from aqueous solution. The significance and adequacy of the model were analyzed using analysis of variance (ANOVA). Four independent variables—including catalyst amount (0.1–0.9 g), pH (3.5–9.5), removal time (30–150 s) and dye concentration (10–50 mg/L)—were transformed to coded values and consequently second order quadratic model was built to predict the responses. The result showed that under optimized experimental conditions the removal of RB21 was over 95%.

1. Introduction

The removal of color from textile effluents has drawn attention over the past few years. Even low concentration dyes can have a damaging impact on the quality of the fiber in nutrition and marine vegetation. Due to the deleterious effects of many organic dyes, it is critical to remove them from waste materials (Vijayaraghavan et al., 2009; Xue et al., 2009). One of the common classes of dyes used in industry is reactive dyes. These dyes are typically based on the nitrogen chromophors combined with various types of reactive groups, such as vinyl sulfone, chlorotriazine, trichloropyrimidine, difluorochloropyrimidine. Considering their carcinogenic effects, it is essential to remove such dyes inasmuch as no damage is caused to reservoirs (Djordjevic et al., 2011).

Among the numerous dye removal techniques, adsorption (e.g. activated carbon and biological treatment) is now preferable as it can be used to remove various types of coloring

* Corresponding author at: Young Researchers and Elites Club, North Tehran Branch, Islamic Azad University, Tehran, Iran. Tel.: +98 9128468020.
E-mail address: mina.moghri@yahoo.com (M. Moghri).
Peer review under responsibility of King Saud University.

ELSEVIER Production and hosting by Elsevier

http://dx.doi.org/10.1016/j.arabjc.2014.11.060
1878-5352 © 2014 The Authors. Production and hosting by Elsevier B.V. on behalf of King Saud University.

materials. Nonetheless, there are some disadvantages associated with each of these techniques. For example, activated carbon adsorption only transfers the dyes from the liquid phase to solid phase. The biological process is difficult to start up and control. The organic compound in the wastewater cannot be degraded completely by the biological process and as a result, the total cost can increase because of the need for further treatment (Lin et al., 2008; Perery et al., 2002).

In recent years, Zero-Valent Iron (ZVI) has been applied as an alternative method to reduce organic pollutants. This catalyst functions well as a non-toxic, reducing agent which is powerful, easy-to-produce and cheap. ZVI in low iron concentration remaining in the sludge has no requirement for further treatment of effluents and is easily recycled from the spent iron powder by magnetism (Shu et al., 2007). ZVI is effectively used to reduce wide range of common environmental contaminates such as chlorinated compounds, nitro aromatic compounds, pesticides, nitrates, heavy metals and dyes (Cong et al., 2010; Efecan et al., 2009; Garg et al., 2003; Liao et al., 2007; Lien and Zhang, 2001; Shimizu et al., 2011; Shu et al., 2010; Üzüm et al., 2008; Xi et al., 2010; Yang and Lee, 2005). Production of iron nanoparticles was improved by several synthetic methods. The borohydride reduction of Fe (II) OR Fe (III) ions in aqueous media is the most efficient method to generate ZVI nanoparticles (Sun et al., 2007). In this paper, Reactive Blue 21 (RB21) was selected to test. RB21 contains copper phthalocyanine chromophore vinyl-sulfonic acid, which is toxic (de Jesus da Silveira Neta et al., 2011) and it has been removed from wastewater with various methods. For example, Silvia et al. removed RB21 from wastewater by using turnip peroxidase (Silva et al., 2012) or Sismanoglu et al. removed it with adsorption method (Sismanoglu et al., 2010).

In customary optimization methods, one-variable-at-a-time, which is used for monitoring the influence of operational parameters, is time-consuming and costly. Therefore, the multivariate statistic techniques were used to optimize the effective parameters. Response surface methodology (RSM) is a powerful statistical technique to investigate the interactive effects between several factors at different levels. It has been successfully employed to optimize removal of pollutants (Kumar et al., 2013; Pang et al., 2011; Kalantari et al., 2014). The main advantage of RSM is that it reduces the number of experimental runs, and saves energy, time, and the materials consumed. The observed results (actual responses) were fitted with a polynomial model in the vicinity of the optimum responses. Then, the model made a relationship between the responses and the variables. The optimum values of the responses and the variables are calculated by the model (Abdollahi et al., 2012; Gunawan et al., 2005; Masoumi et al., 2013).

2. Experimental

2.1. Materials and apparatus

Reactive Blue 21 (Molecular formula ($C_{40}H_{26}CuN_{10}O_{16}S_6$), Molecular Weight 1159.62 g/mol, λ_{max} 614 nm), was obtained from ALVAN SABET company, Iran, and was used without any further purification (Fig. 1 shows the chemical structure of RB21.). Sodium Borohydride ($NaBH_4$), Iron (III) chloride ($FeCl_3{\cdot}6H_2O$), Acetone, HCl and NaOH were obtained from Merck. Deionized distilled water (DDW) was used in all experiments. The amount of residual RB21 was analyzed by double beam UV–Vis spectrometer (Cary 100-varian).

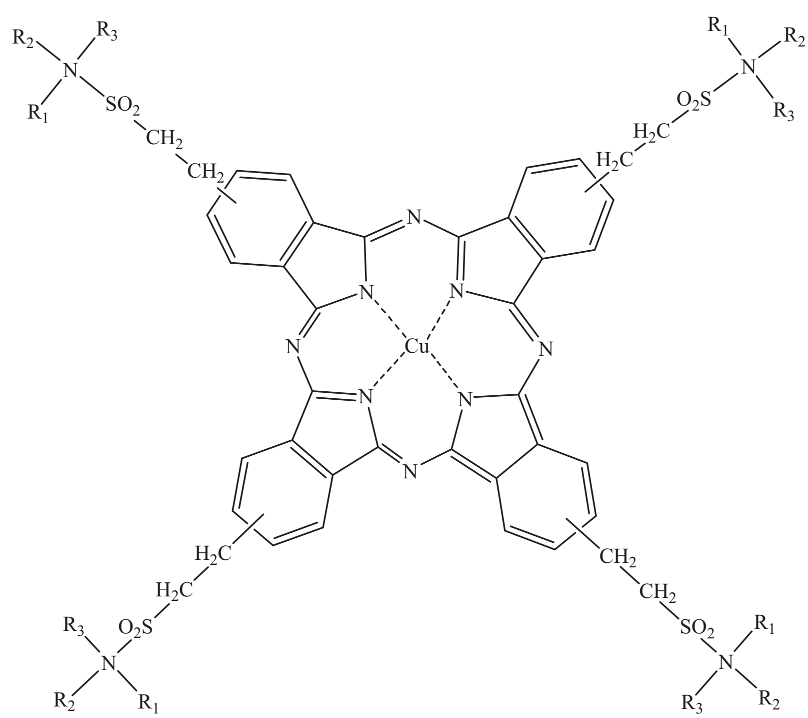

Figure 1 Molecular structure of Reactive Blue 21.

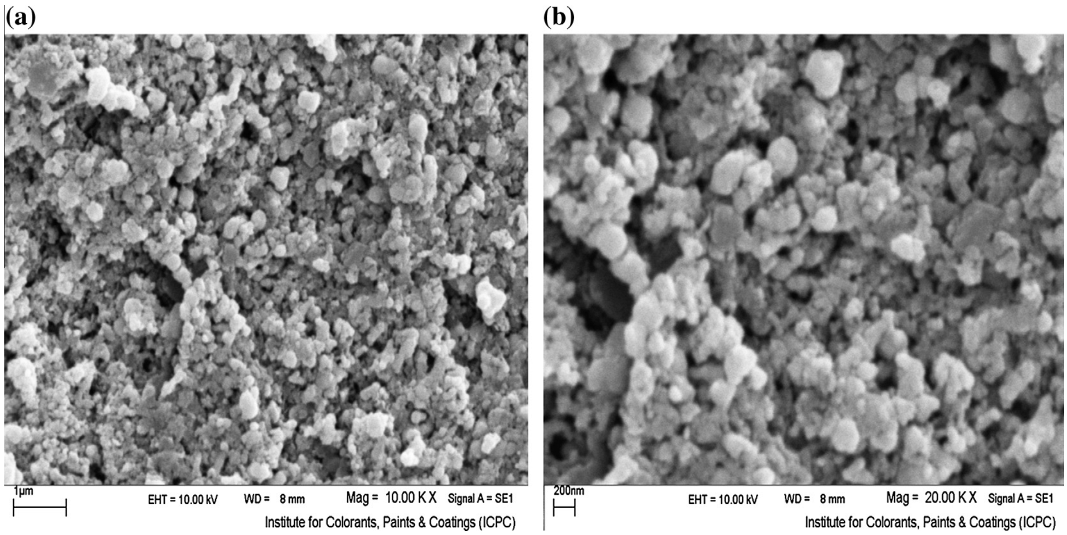

Figure 2 Scanning electron micrograph (SEM) of iron nanoparticles: (a) 10.000 KX; (b) 20.000 KX.

2.2. Synthesis of Nano ZVI and characterization by SEM and XRD

Nano-scale Zero-Valent Iron particles used in this study were chemically synthesized in aqueous solution via the reduction of ferric iron by sodium borohydride (Frost et al., 2010; Liao et al., 2007). The experiments were carried out in the room temperature by applying N_2 atmosphere gas. In this work, $NaBH_4$ solution (0.3 M) was gradually dropped into $FeCl_3 \cdot 6H_2O$ solution (0.1 M) and the solution was mixed by a tunable mechanical stirrer at 415 rpm. The resulting reaction can be given as below (Eq. (1)) (Sun et al., 2007):

$$4Fe^{3+}_{(aq)} + 3BH^{-}_{4(aq)} + 9H_2O \rightarrow 4Fe^{0}_{(s)} + 3H_2BO^{-}_{3(aq)} + 12H^{+}_{(aq)} + 6H_{2(g)} \quad (1)$$

Black particles of NZVI, as a form of sedimentation, appeared immediately after introducing the first drop of $NaBH_4$ solution. The generated iron particles were separated by vacuum filtration and washed by DDW. In order to stabilize NZVI against immediate oxidation, the solid was washed at least two times with 98% acetone.

Morphology and the sizes of NZVI particles were identified by scanning electron microscope (SEM) (LEO-1455VP, England) as shown in Fig. 2. This image demonstrates that the iron particles are in the form of nano-spheres and they exist in contact with one another forming chains with diameters of < 100 nm.

XRD analysis of newly-synthesized iron nanoparticles was carried out with Philips, PW3050, the XRD pattern is shown in Fig. 3 indicating that the Zero-Valent Iron has only a characteristic 2θ value of 44.7°, and no signals for iron oxides with a 2θ value of 36° were found. It also indicates that the ZVI is mainly seen in the sample.

The treatment was carried out by adding 0.1–0.9 g NZVI into 50 ml dye solution.

2.3. Experimental design and data analysis

In the present study, a five-level-four-factor Central Composite Rotatable Design, which is a widely used form of RSM,

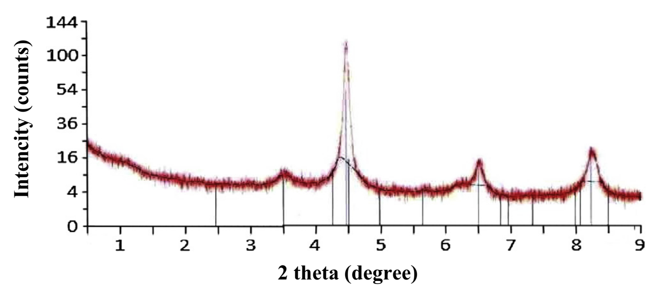

Figure 3 XRD pattern of Nano Zero-Valent Iron (NZVI) particles.

was employed for optimization of RB21 removal. The procedure of optimization has been represented in the form of a flowchart as shown in Fig. 4. A set of 30 experiments were designed to optimize by Nano ZVI catalyst. Four independent variables called catalyst dosage, pH, removal time and initial concentration were investigated and each variable in the design was studied at five different coded levels (Table 1). The variables were coded according to the following equation (Eremia et al., 2008):

$$x_i = \frac{X_{i-}X_0}{\Delta X_i} \quad (2)$$

where x_i is the independent variable coded value, X_i, X_0 are independent variable real value where X_0 is on the center point; ΔX_i is the step changing value (Eremia et al., 2008). The influence of individual factor from the experiments and their performance at optimum condition by using RSM approach were analyzed by the software *Design Expert* (version 6.0.6) (Gunawan et al., 2005). The reliable way to evaluate the quality of the model fitted is to apply analysis of variance (ANOVA) (Khataee et al., 2011). Data collected from various mathematical models (Linear, two factorial interaction (2FI), quadratic and cubic) as well as ANOVA prove that the reaction of decolorization was most properly demonstrated with a quadratic polynomial model and the quadratic equation for the variable is in the following form (Eq. (3)):

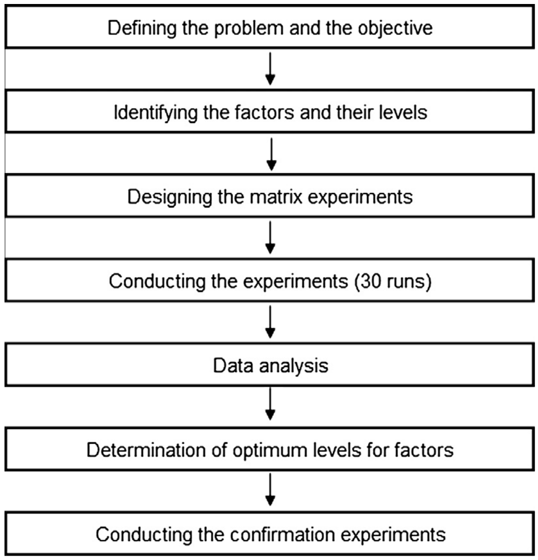

Figure 4 The procedure of using RSM for optimization.

Table 1 Levels and code variables used for RB21 removal.

Variables	Symbol coded	Levels				
		−2	−1	0	1	2
Catalyst amount (g)	X_1	0.1	0.3	0.5	0.7	0.9
pH	X_2	3.5	5	6.5	8	9.5
Removal time (s)	X_3	30	60	90	120	150
Dye concentration (mg/L)	X_4	10	20	30	40	50

$$\left[Y = \beta_0 + \sum_{i=1}^{4}\beta_i x_i + \sum_{i=1}^{4}\beta_{ii} x_i^2 + \sum_{i=1}^{3}\sum_{j=i+1}^{4}\beta_{ij} x_i x_j + \varepsilon\right] \quad (3)$$

where Y (dye reduction %) is the predicted response, β_0 is intercept coefficient, β_i represents the coefficient of linear parameters, β_{ii} and β_{ij} are the interaction coefficients of quadratic and second order, respectively. X_i and X_j represent the coded independent variables (Bezerra et al., 2008; Cho and Zoh, 2007; Eremia et al., 2008; Fu et al., 2007). As it is illustrated in Table 2, the F-value is calculated for each sort of model, and the topmost order model with significant terms is normally selected. The significance is evaluated as F-value being calculated out of the data exceeding a theoretical value (Muralidhar et al., 2001). To determine the extreme values of the variables, we carried out preparatory experiments.

Table 3 The design of RSM and its actual and predicted values.

Run	X_1	X_2	X_3	X_4	Removal (%)	
					Experimental	Predicted
1	−1	−1	−1	−1	70.34	73.49
2	1	−1	−1	−1	92.07	90.66
3	−1	1	−1	−1	79.45	79.74
4	1	1	−1	−1	89.04	90.60
5	−1	−1	1	−1	80.20	80.18
6	1	−1	1	−1	95.04	97.35
7	−1	1	1	−1	85.01	86.43
8	1	1	1	−1	93.40	97.29
9	−1	−1	−1	1	73.67	71.77
10	1	−1	−1	1	85.64	85.38
11	−1	1	−1	1	74.90	70.66
12	1	1	−1	1	78.30	77.95
13	−1	−1	1	1	87.89	84.77
14	1	−1	1	1	99.40	98.37
15	−1	1	1	1	79.90	83.66
16	1	1	1	1	93.30	90.95
17	−2	0	0	0	68.95	69.48
18	2	0	0	0	94.90	93.93
19	0	−2	0	0	81.50	82.84
20	0	2	0	0	83.45	81.67
21	0	0	−2	0	75.10	76.89
22	0	0	2	0	98.80	96.58
23	0	0	0	−2	98.54	93.15
24	0	0	0	2	80.14	85.09
25	0	0	0	0	94.90	96.83
26	0	0	0	0	94.95	96.83
27	0	0	0	0	98.85	96.83
28	0	0	0	0	97.00	96.83
29	0	0	0	0	99.50	96.83
30	0	0	0	0	95.80	96.83

3. Results and discussion

3.1. Model fitting and statistical analysis

Experimental data to remove RB-21 from wastewater are given in Table 3 along with the predicted values. The data were fitted with various models and their subsequent ANOVA showed that reaction of RB21 removal was most suitably described by quadratic polynomial model. The final model to predict the percentage of RB21 removal by NZVI is shown in Eq. (4):

$$\begin{aligned}\%Y = {} & 96.83 + 6.11X_1 - 0.29X_2 + 4.92X_3 - 2.01X_4 \\ & - 3.78X_1^2 - 3.64X_2^2 - 2.53X_3^2 - 1.93X_4^2 - 1.58X_1X_2 \\ & - 0.89X_1X_4 - 1.84X_2X_4 + 1.58X_3X_4 \end{aligned} \quad (4)$$

Table 2 Statistical parameters for sequential models.

Source	Sum of square	DF	Mean square	F-value	Prob > F	Remarks
Mean vs total	2.288E+005	1	2.288E+005	–		
Linear vs mean	1577.99	4	394.50	9.16	0.0001	–
2FI vs linear	154.17	6	25.70	0.53	0.7795	–
Quadratic vs 2FI	753.91	4	188.48	16.73	< 0.0001	Suggested
Cubic vs quadratic	147.48	8	18.44	5.99	0.0145	Aliased
Residual	21.55	7	3.08	–	–	–
Total	2.315E+005	30	7715.21	–	–	–

Table 4 Analysis of variance (ANOVA) results of quadratic model to remove RB21.

Source	Sum of square	DF	Mean square	F-value	P-value	
Model	2478.53	12	2478.53	19.89	< 0.0001	Significant
X_1	897.07	1	897.07	86.37	< 0.0001	
X_2	2.07	1	2.07	0.2	0.6609	
X_3	581.45	1	581.45	55.98	< 0.0001	
X_4	97.41	1	97.41	9.38	0.0071	
X_1^2	392.19	1	392.19	37.76	< 0.0001	
X_2^2	364.19	1	364.19	35.06	< 0.0001	
X_3^2	174.89	1	174.89	16.84	0.0007	
X_4^2	101.92	1	101.92	9.81	0.0061	
X_1X_2	39.91	11	39.91	3.84	0.0666	
X_1X_4	12.73	1	12.73	1.23	0.2837	
X_2X_4	54.21	1	54.21	5.22	0.0355	
X_3X_4	39.78	1	39.78	3.83	0.067	
Residual	176.57	17	176.57			
Lack of fit	157.01	12	157.01	3.34	0.0958	Not significant

R^2 = 0.9335, Adj-R^2 = 0.8866, Adequate precision = 13.620.

where X_1 is amount of catalyst, X_2 the pH, X_3 the removal time, X_4 the initial concentration of RB21.

F-value calculated from the data (19.89) was higher than tabular value. ANOVA and values of the factors are shown in Table 4. Coefficient of determination, R^2, always lies between 0 and 1 (Priya and Kanmani, 2011). (However, Masoumi et al., (2011) stated that if R^2 value lies between 0.90 and 1.00, the fitted regression equation is considered as a model having a high correlation.)

In this study, R^2 of the model was 0.9335. It indicates 93.35% of the experimental data and predicted data can be explained by the model. In addition, the value of adjusted determination coefficient Adj R^2 = 0.8866 was also satisfactory, confirming the significance of the model.

The value of coefficient of variation (CV = 3.69%) implied that there is good validity in the experimental data and the model. It can be considered reasonably reproducible if its CV is not greater than 10%. A lower value of CV clearly showed a high degree of precision. The model also showed adequate precision by measurement of signal to noise ratio. The ratio greater than 4 is desirable. Thus, a ratio of 13.620 indicated an adequate signal (Masoumi et al., 2011).

Fig. 5 indicates a plot of predicted value vs actual value of percentage removal from response surface design, where the coefficient of determination (R^2) was (0.9335) and indicated a good agreement with model. In the meanwhile, the residual plots represent appropriateness of the model and correlation of the data (Fig. 6). The residuals are randomly scattered in a constant width band about the zero line. The root mean squares error (RMSE = 2.42) and the absolute average deviation (AAD = 2.30) were determined. The RMSE and AAD are calculated by the following equations:

$$\mathrm{RMSE} = \left(\frac{1}{n}\sum_{i=1}^{n}(y_{ia-}y_p)^2\right)^{1/2} \quad (5)$$

$$\mathrm{AAD} = \frac{\sum_i^n(|y_p - y_{ia}|/y_{ia})}{n} \times 100 \quad (6)$$

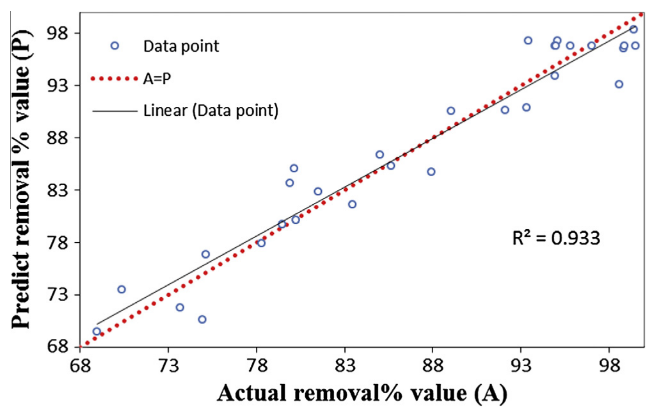

Figure 5 Scatter plot of predicted removal % value vs actual removal % value from RSM design.

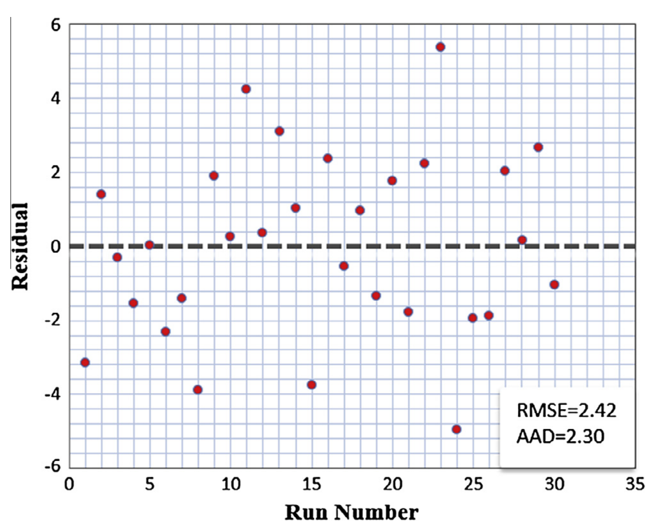

Figure 6 Residual plot of model.

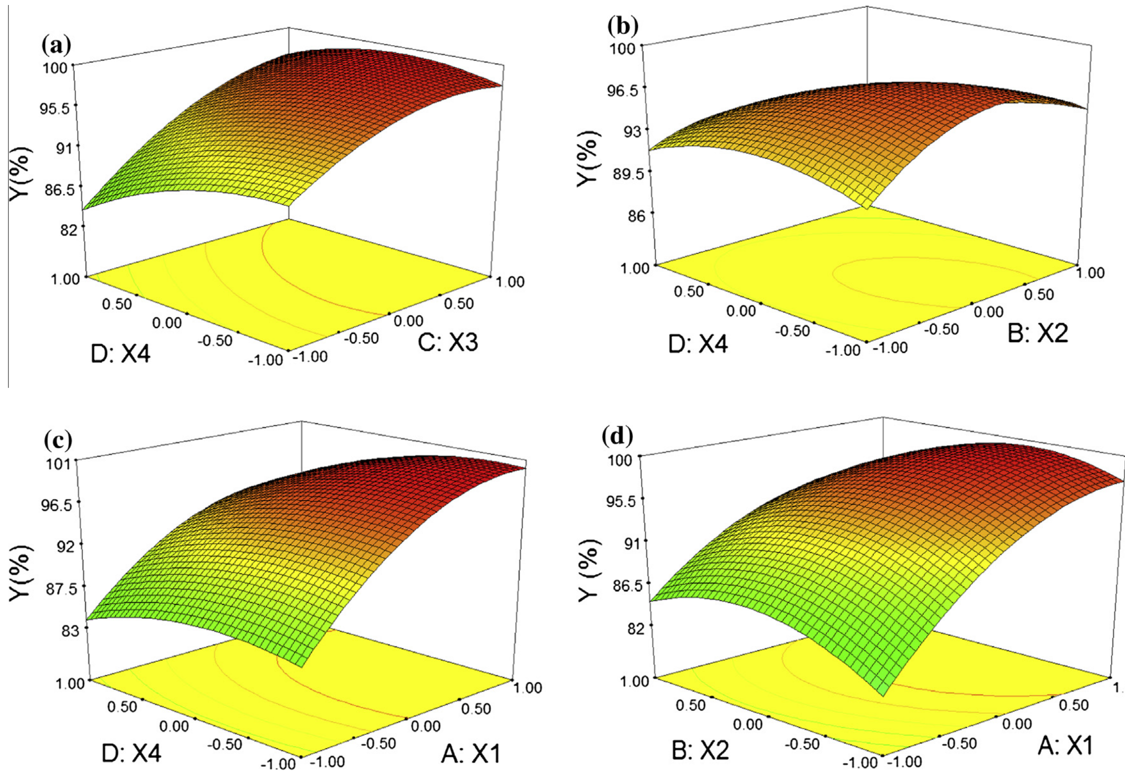

Figure 7 Response surfaces plot. (a) Interaction plot of removal time (X_3) and dye concentration (X_4). (b) Interaction plot of pH (X_2) and dye concentration (X_4). (c) Interaction plot of catalyst amount (X_1) and dye concentration (X_4). (d) Interaction plot of catalyst amount (X_1) and pH (X_2).

Table 5 Optimum conditions derived by RSM for removal of RB21 dye.

Exp.	Optimal conditions				Removal (%)		
	X_1	X_2	X_3	X_4	Actual	Predicted	RSE %
1	0.34	6.33	120	40	88.46	90.05	1.13
2	0.34	6.31	120	40	92.03	90.59	1.59
3	0.35	6.73	120	37.5	90.44	91.58	1.25

where n is the number of experiments, y_p is the predicted value obtained from the RSM, and y_{ia} is the actual value (Masoumi et al., 2011).

3.2. Interaction between influencing factors

The three-dimensional response surface plots were used to determine the interaction between the four variables. The results are displayed in Fig. 7. The optimum situation of the relative variables is similar to the coordinates of central point in the upmost level in each of these figures. Fig. 7a represents that RB21 removal increases as time passes during reaction and decreases with the increase of dye concentration (while keeping other variables at a constant level). The reason is that in dye's low concentrations, there is a close relation between surface active sites and the total dye molecules. Consequently, all molecules stick to NZVI surface and then are removed from the solution. However, there is not enough space for all molecules in high concentration of dye.

Fig. 7b shows the response surface plot of RB21 removal as a function of initial concentration of RB21 and pH. The pH was also one of the important factors in RB21 removal rate. More than 80% of dye removal by ZVI was observed around the neutral range of pH 4–9 (Shu et al., 2007). The removal rate increased at pH value below 9. This case can be ascribed to the fact that lower pH_{ZPC} ($< pH_{ZPC} \sim 8.3$) is favorable for removal of anionic dye on the iron surface (Fan et al., 2009) but extremely basic or acidic conditions gave poor removal results. These results agree with previous reports on the ZVI transformation of dyes (Fan et al., 2009; Shu et al., 2007). As it is obvious from Fig. 7b RB21 removal increased at weak acidic range and decreased at extremely basic or acidic conditions within increase initial concentration of RB21. Fig. 7c demonstrates that with an increased amount of the catalyst and a decreased dye concentration, RB21 removal increases. Fig. 7d shows the effect of the catalyst amount and pH on RB21 removal. This diagram clearly states that around the neutral range of pH (lower pH_{zpc}) with an increased catalyst amount, the efficiency of RB21 removal increases. The surface charge of NZVI under pH_{zpc} is positive and it helps the removal of anionic compounds such as reactive dyes.

3.3. Optimization of reaction and model validation

To confirm the model's adequacy for predicting maximum RB21 removal, three additional experiments were used. Such optimum conditions were performed and are now presented in Table 5.

The optimum reaction parameters were a catalyst amount of 0.5 g, initial concentration of 30 ppm, pH of 6.5, and removal time of 90s. All the optimum conditions can be used to produce high percentage Reactive Blue 21 removal. The desired value of the residual standard error (1.25) is also obtained from the optimum condition of RSM experimental design. Comparison of predicted and actual values revealed good correspondence between them, implying that the empirical model derived from design expert software can describe the relationship between the factors and outputs.

4. Conclusion

ZVI appeared to be a very active catalyst for removal of textile dye from aqueous solution. A central composite design was applied to provide the experimental conditions for dye removal. In the present study, removal time, initial concentration of RB21, the amount of catalyst, and pH were the most significant effects on the removal of RB21. Results show that response surface methodology is one of the most useful methods to optimize the experimental conditions for the removal of RB21 from wastewater. According to the analysis results, 0.5 g ZVI catalyst, natural pH, 90s removal time, and initial concentration of RB21 30 mg/L, were formed the optimum conditions. The model validation results (R^2 = 0.9335, RMSE = 2.42, AAD = 2.30) were suggested for the adequacy of the developed model. The quadratic equation developed in this study shows the presence of a high correlation between the values predicted by experimental design and the ones obtained experimentally. Analysis of variance depicts the accuracy of the model by using high *F*-value (19.89), very low *P*-value ($<$0.0001), non-significant lack of fit, the coefficient of determination (0.9335) and the adequate precision (13.620). Consequently useful information about this alternative wastewater technology was obtained by considering the effects of NZVI on optimizing the potential parameters of Reactive Blue 21 dye removal.

References

Abdollahi, Y., Zakaria, A., Abdullah, A.H., Masoumi, H.R.F., Jahangirian, H., Shameli, K., Rezayi, M., Banerjee, S., Abdollahi, T., 2012. Semi-empirical study of ortho-cresol photo degradation in manganese-doped zinc oxide nanoparticles suspensions. Chem. Cent. J. 6, 88.

Bezerra, M.A., Santelli, R.E., Oliveira, E.P., Villar, L.S., Escaleira, L.A., 2008. Response surface methodology (RSM) as a tool for optimization in analytical chemistry. Talanta 76, 965–977.

Cho, I.H., Zoh, K.D., 2007. Photocatalytic degradation of azo dye (Reactive Red 120) in TiO_2/UV system: optimization and modeling using a response surface methodology (RSM) based on the central composite design. Dyes Pigm. 75, 533–543.

Cong, X., Xue, N., Wang, S., Li, K., Li, F., 2010. Reductive dechlorination of organochlorine pesticides in soils from an abandoned manufacturing facility by zero-valent iron. Sci. Total Environ. 408, 3418–3423.

De Jesus da Silveira Neta, J., Costa Moreira, G., da Silva, C.J., Reis, C., Reis, E.L., 2011. Use of polyurethane foams for the removal of the Direct Red 80 and Reactive Blue 21 dyes in aqueous medium. Desalination 281, 55–60.

Djordjevic, D., Stojkovic, D., Djordjevic, N., Smelcerovice, M., 2011. Thermodynamic of reactive dye adsorption from aqueous solution on the ashes from city heating station. Ecol. Chem. Eng. 18, 527–535.

Efecan, N., Shahwan, T., Eroğlu, A.E., Lieberwirth, I., 2009. Characterization of the uptake of aqueous Ni^{2+} ions on nanoparticles of zero-valent iron (nZVI). Desalination 249, 1048–1054.

Eremia, S.A.V., Chevalier-Lucia, D., Radu, G.L., Marty, J.L., 2008. Optimization of hydroxyl radical formation using TiO_2 as photocatalyst by response surface methodology. Talanta 77, 858–862.

Fan, J., Guo, Y., Wang, J., Fan, M., 2009. Rapid decolorization of azo dye methyl orange in aqueous solution by nanoscale zerovalent iron particles. J. Hazard. Mater. 166, 904–910.

Frost, R.L., Xi, Y., He, H., 2010. Characterization of palygorskite supported zero-valent iron and its application for methylene blue adsorption. J. Colloid Interface Sci. 341, 153–161.

Fu, J., Zhao, Y., Wu, Q., 2007. Optimising photoelectrocatalytic oxidation of fulvic acid using response surface methodology. J. Hazard. Mater. 144, 499–505.

Garg, V.K., Gupta, R., Yadav, A.B., Kumar, R., 2003. Dye removal from aqueous solution by adsorption on treated sawdust. Bioresour. Technol. 89, 121–124.

Gunawan, E.R., Basri, M., Rahman, M.B.A., Salleh, A.B., Rahman, R.N.Z.A., 2005. Study on response surface methodology (RSM) of lipase-catalyzed synthesis of palm-based wax ester. Enzyme Microb. Technol. 37, 739–744.

Kalantari, K., Ahmad, M.B., Masoumi, H.R.F., Shameli, K., Basri, M., Khandanlou, R., 2014. Rapid adsorption of heavy metals by Fe_3O_4/talc nanocomposite and optimization study using response surface methodology. Int. J. Mol. Sci. 15, 12913–12927.

Khataee, A., Zarei, M., Fathinia, M., Jafari, M.K., 2011. Photocatalytic degradation of an anthraquinone dye on immobilized TiO_2 nanoparticles in a rectangular reactor: destruction pathway and response surface approach. Desalination 268, 126–133.

Kumar, S.N.A., Ritesh, S.K., Sharmila, G., Muthukumaran, C., 2013. Extraction optimization and characterization of water soluble red purple pigment from floral bracts of *Bougainvillea glabra*. Arabian J. Chem. 10. http://dx.doi.org/10.1016/j.arabjc.2013.07.047.

Liao, C.J., Chung, T.L., Chen, W.L., Kuo, S.L., 2007. Treatment of pentachlorophenol-contaminated soil using nano-scale zero-valent iron with hydrogen peroxide. J. Mol. Catal. A: Chem. 265, 189–194.

Lien, H.L., Zhang, W., 2001. Nanoscale iron particles for complete reduction of chlorinated ethenes. Colloids Surf. A Physicochem. Eng. Asp. 191, 97–105.

Lin, Y.T., Weng, C.H., Chen, F.Y., 2008. Effective removal of AB24 dye by nano/micro-size zero-valent iron. Sep. Purif. Technol. 64, 26–30.

Masoumi, H.R.F., Kassim, A., Basri, M., Abdullah, D.K., 2011. Determining optimum conditions for lipase-catalyzed synthesis of triethanolamine (TEA)-based Esterquat cationic surfactant by a Taguchi robust design method. Molecules 16, 4672–4680.

Masoumi, H.R.F., Basri, M., Kassim, A., Abdullah, D.K., Abdollahi, Y., Abd Gani, S.S., Rezayee, M., 2013. Statistical optimization of process parameters for lipase-catalyzed synthesis of triethanolamine-based Esterquats using response surface methodology in 2-liter bioreactor. Sci. World J. 2013, 9.

Muralidhar, R.V., Chirumamila, R.R., Marchant, R., Nigam, P., 2001. A response surface approach for the comparison of lipase production by *Candida cylindracea* using two different carbon sources. Biochem. Eng. J. 9, 17–23.

Pang, Y.L., Abdullah, A.Z., Bhatia, S., 2011. Optimization of sonocatalytic degradation of Rhodamine B in aqueous solution in the presence of TiO_2 nanotubes using response surface methodology. Chem. Eng. J. 166, 873–880.

Perery, J.R., Chiu, P.C., Huang, C.P., Cha, D.K., 2002. Water Environ. Res. 74, 221.

Priya, R., Kanmani, S., 2011. Optimization of photocatalytic production of hydrogen from hydrogen sulfide in alkaline solution using response surface methodology. Desalination 276, 222–227.

Shimizu, A., Tokumura, M., Nakajima, K., Kawase, Y., 2011. Phenol removal using zero-valent iron powder in the presence of dissolved oxygen: roles of decomposition by the Fenton reaction and adsorption/precipitation. J. Hazard. Mater. 201–202, 60–67.

Shu, H.Y., Chang, M.C., Yu, H.H., Chen, W.H., 2007. Reduction of an azo dye Acid Black 24 solution using synthesized nanoscale zerovalent iron particles. J. Colloid Interface Sci. 314, 89–97.

Shu, H.Y., Chang, M.C., Chen, C.C., Chen, P.E., 2010. Using resin supported nano zero-valent iron particles for decoloration of Acid Blue 113 azo dye solution. J. Hazard. Mater. 184, 499–505.

Silva, M.C., Corrêa, A.D., Amorim, M.T.S.P., Parpot, P., Torres, J.A., Chagas, P.M.B., 2012. Decolorization of the phthalocyanine dye reactive blue 21 by turnip peroxidase and assessment of its oxidation products. J. Mol. Catal. B Enzym. 77, 9–14.

Sismanoglu, T., Kismir, Y., Karakus, S., 2010. Single and binary adsorption of reactive dyes from aqueous solution onto clinoptilolite. J. Hazard. Mater. 184, 164–169.

Sun, Y.P., Li, X.Q., Zhang, W.X., Wang, H.P., 2007. A method for the preparation of stable dispersion of zero-valent iron nanoparticles. Colloids Surf. A Physicochem. Eng. Asp. 308, 60–66.

Üzüm, C., Shahwan, T., Eroğlu, A., Lieberwirth, I., Scott, T., Hallam, K., 2008. Application of zero-valent iron nanoparticles for the removal of aqueous Co^{2+} ions under various experimental conditions. Chem. Eng. J. 144, 213–220.

Vijayaraghavan, K., Won, Sung Wook, Yun, Yeoung-Sang, 2009. Treatment of complex Remazol dye effluent using sawdust- and coal-based activated carbons. J. Hazard. Mater. 167, 790–796.

Xi, Y., Mallavarapu, M., Naidu, R., 2010. Reduction and adsorption of Pb^{2+} in aqueous solution by nano-zero-valent iron—A SEM, TEM and XPS study. Mater. Res. Bull. 45, 1361–1367.

Xue, Y., Hou, H., Zhu, S., 2009. Adsorption removal of reactive dyes from aqueous solution by modified basic oxygen furnace slag: isotherm and kinetic study. Chem. Eng. J. 147, 272–279.

Yang, G.C.C., Lee, H.L., 2005. Chemical reduction of nitrate by nanosized iron: kinetics and pathways. Water Res. 39, 884–894.